ELSEVIER

Microporous and Mesoporous Materials 20 (1998) 27–37

MICROPOROUS AND MESOPOROUS MATERIALS

Structural investigation of zinc oxide clustering in zeolite A and sodalite

L. Khouchaf [a], M.-H. Tuilier [a], M. Wark [b], M. Soulard [b], H. Kessler [b,*]

[a] *Laboratoire de Physique et de Spectroscopie Electronique (UPRES A7014), Université de Haute-Alsace, Faculté des Sciences et Techniques, 4 rue des Frères Lumière, F-68093 Mulhouse, Cedex, France*

[b] *Laboratoire des Matériaux Minéraux (URA CNRS 428), Ecole Nationale Supérieure de Chimie de Mulhouse, 3 rue A. Werner, F-68093 Mulhouse, Cedex, France*

Received 25 April 1997; received in revised form 9 September 1997; accepted 12 September 1997

Abstract

The formation of small zinc oxide clusters in fully Zn-exchanged LTA zeolite and partially Zn-exchanged sodalite submitted to appropriate thermal treatments was investigated by X-ray absorption spectroscopy at the Zn K-edge. The absence of extraneous ZnO or $ZnAl_2O_4$ particles as well as the changes in the zeolite framework produced by thermal treatments was checked by X-ray diffraction as well as ^{29}Si and ^{27}Al MAS NMR. In all the samples, the Zn cations are tetracoordinated to oxygen. In fully Zn-exchanged zeolite A, the EXAFS spectra result from the contribution of inequivalent Zn^{2+} cations belonging to clusters of different size located in either the sodalite cages or the α-cages. In partially Zn-exchanged sodalite, after calcination, the presence of aluminum belonging to the framework as second neighbors of Zn at 2.86 Å is demonstrated, whereas Zn neighbors of Zn are moved away to 3.39 Å instead of 3.24 Å in crystalline ZnO. The results are consistent with the adsorption on the sodalite framework of clusters involving three Zn cations probably hydrolyzed and belonging either to the same cage or to three adjacent cages.

Keywords: Microporous materials; Nanostructure; X-ray absorption spectroscopy; NMR

1. Introduction

The ion-exchange technique of microporous materials is a promising way of stabilizing nanostructures having a definite particle size. The aluminosilicate framework of as-synthesized zeolites, which is characterized by a negative charge, is often neutralized by sodium cations. The exchange of sodium by transition metals cations, which is extensively used in order to obtain specific sorbents and catalysts [1], can be applied to the growth of nanoparticles. Zeolite materials provide a wide range of pores and cages whose size can be chosen to obtain more or less extended clusters. Thus, the growth of the clusters is determined by the size of the pores present in the host structure. The framework of sodalite [2,3], which is schematized in Fig. 1(a), is exclusively made up of face-sharing truncated octahedra which are confined by six four-membered rings and eight six-membered rings of interconnected $(Si,Al)O_4$ tetrahedra [2,3].

* Corresponding author. Fax: +33 3 89428730; e-mail: H.Kessler@univ-mulhouse.fr

1387-1811/98/$19.00
PII S1387-1811(97)00003-6

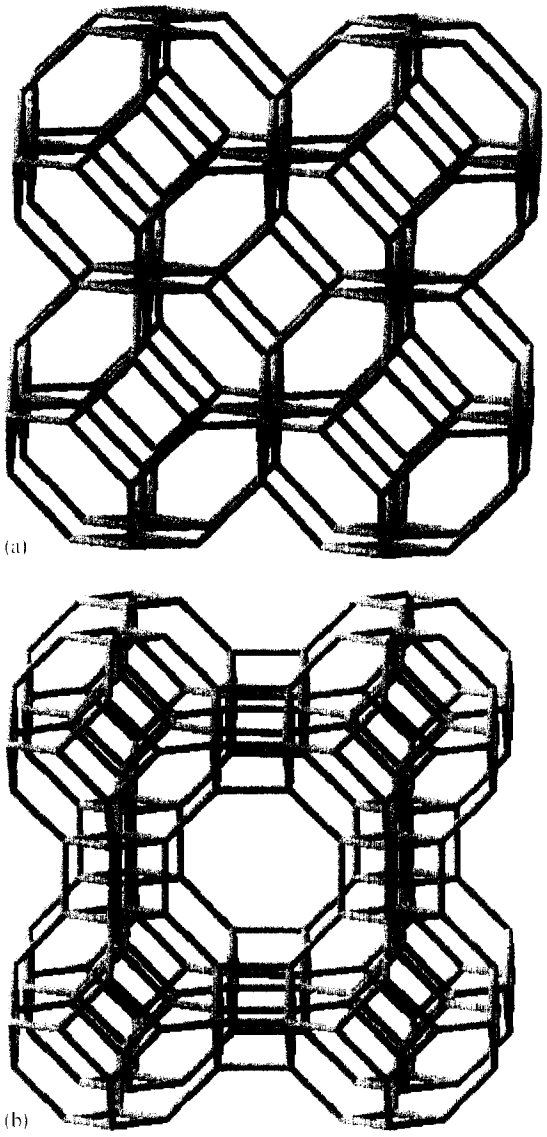

Fig. 1. Schematic diagram of (a) sodalite and (b) zeolite A structures.

The cavities, namely the sodalite cages, have a very small inner diameter of 6.6 Å [2,3]. The ion-exchange of aluminosilicate sodalite by Zn^{2+} cations leads to the partial exchange of sodium ions present in the truncated octahedral cages. On the other hand, the inclusion of small semiconductor particles in sodalite has been achieved by direct synthesis [4]. The structure of zeolite A [Fig. 1(b)] is derived from sodalite by generating double four-membered rings between neighboring sodalite cages. The lattice displays, in addition to sodalite cages, larger cavities with an inner diameter of 11.3 Å, so-called α-cages, and smaller ones, formed by double four-membered rings, with an inner diameter of about 2.7 Å. Zeolite A can be fully Zn-exchanged. In the early 1980s, the crystallographic structure of Zn-exchanged zeolite A was determined by single-crystal X-ray diffraction (XRD) [5,6], but the presence of three kinds of cavities gives rise to an inhomogeneous compound with various sites for the Zn^{2+} cations. The significance of Zn-exchanged zeolites stems from the semiconducting properties of ZnO, which are modified for small clusters. Indeed, the optical properties of nanometer-sized materials which have been determined by reflectance and luminescence spectra, and UV–visible absorption spectroscopy [7,8] are very attractive for applications in the field of optics and photocatalysis [9,10].

X-ray absorption spectroscopy (XAS) allows us to complete the XRD structural analysis since it allows a separate analysis of the Zn environment in the inserted particles and a determination of the geometrical arrangement of the clusters, irrespective of the host lattice. Extended X-ray absorption fine structure (EXAFS) has been used together with XRD in the structural determination of CdSe semiconductor particles obtained by ion-exchange of zeolite Y [11]. The EXAFS study of selenium inserted in Na-mordenite has recently shown that the information on the structure of the chains inserted in the zeolite framework is greatly improved if the analysis is extended to the second and third coordination shells around the inserted element [12].

The aim of this work is to obtain more accurate structural information on the ultra-small clusters that are present in the sodalite cages of Zn-exchanged zeolite A, by investigating similar clusters inserted in aluminosilicate sodalite. These clusters are presumed to interact strongly with the aluminosilicate framework [8].

The preparation of fully Zn-exchanged LTA zeolite and partially Zn-exchanged sodalite is described here. Thermal treatments at various temperatures were applied to both exchanged materials. EXAFS analysis at the Zn K-edge including

the first, second and third shells of neighbors around Zn was performed on Zn-exchanged sodalite and zeolite A and revealed a modification in the former depending on the treatment.

2. Experimental

2.1. Sample preparation

2.1.1. Zn^{2+}-exchanged zeolite A

The starting material was zeolite Na-A, purchased from KCB Bitterfeld (Germany). The exchange of Zn^{2+} for Na^+ ions was performed by using twice a 0.05 M zinc chloride solution at room temperature for 4 h. A liquid/solid mass ratio of 100 was chosen. The control of the pH value during the zinc exchange of zeolite A ensured that no or only very small amounts of $Zn(OH)_2$ were precipitated on the outer crystals during this procedure. Indeed, the measured pH value was always higher than 5.8. Taking into account earlier results [8,13], the precipitation of considerable amounts of zinc hydroxide should lead to a drop of the pH below 5.5. The resulting compound dried at 80°C is referred to as the AZEO80 sample. Part of the AZEO80 sample was calcined in air with a heating rate of 2°C/min up to 540°C for 5 h, giving the AZEO540 sample. The AZEO600 sample results from the calcination of another part of AZEO80 at 600°C for 5 h at the much lower rate of 0.5°C/min.

The samples were then cooled and subsequently rehydrated under an atmosphere of controlled humidity (over a saturated NH_4Cl solution). The Si, Al, Na and Zn contents were determined by atomic absorption spectroscopy, using a VARIAN model AA6 instrument. The ion-exchange degree of the three samples after complete dissolution of the solid phase was found to be $95\pm2\%$ for AZEO80 and $93\pm2\%$ for AZEO540 and AZEO600. The latter value is lower than the former but remained within experimental error. The amount of water was determined by thermogravimetry. The formula per pseudo-unit cell is $Na_{0.8}Zn_{5.6}Si_{12}Al_{12}O_{48}\cdot xH_2O$, with $x=30$ for AZEO80 and $x=28$ for AZEO540 and AZEO600.

2.1.2. Zn^{2+}-exchanged sodalite

Zn was incorporated via different routes, namely (i) by cation exchange as for the zeolite A samples and (ii) by direct synthesis.

(i) Na sodalite was prepared from a reaction gel with the following molar composition: $3.4SiO_2{:}1Al_2O_3{:}33Na_2O{:}70H_2O$. Crystallization was achieved by heating at 110°C for 3 days. After checking the purity of the phase by XRD, the product was exchanged twice with a $ZnCl_2$ solution. The sample SOD600 was obtained by calcination at 600°C for 5 h and rehydration (see above). The formula is found to be $Na_{4.2}Zn_{0.9}Si_6Al_6O_{24}\cdot xH_2O$, with $x=12$ and $x=4$ before and after calcination, respectively.

(ii) The starting mixture used for the direct synthesis was: $2.2SiO_2{:}1Al_2O_3{:}7Na_2O{:}0.8ZnO{:}110H_2O$. The reactants were sodium metasilicate pentahydrate (Prolabo), sodium aluminate (Carlo-Erba), sodium hydroxide (Fluka, purum) and zinc acetate dihydrate (Fluka, purum). The crystallization was carried out in a PTFE-lined stainless steel autoclave at 110°C for 10 days. After reaction, the product was recovered by filtration, washed and dried at 80°C and rehydrated, thus yielding a sample called SOD80. Part of that product was calcined at 400°C for 5 h with a heating rate of 0.5°C/min and rehydrated under the usual conditions to give the SOD400 sample. The composition of SOD80 and SOD400 is $Na_{4.2}Zn_{0.9}Si_6Al_6O_{24}\cdot xH_2O$ with $x=12$ and $x=2$ for SOD80 and SOD400, respectively.

2.2. X-ray diffraction

The XRD diffractograms of the samples were obtained by using Cu Kα radiation on a Philips PW1800 diffractometer with variable entrance slit.

2.3. ^{29}Si and ^{27}Al MAS NMR

The spectra of ^{29}Si and ^{27}Al MAS NMR were recorded on a Bruker MSL 300 spectrometer. The recording conditions were: for ^{29}Si, frequency = 59.63 MHz, pulse width = 5 μs, recycle time = 30 s, spinning rate = 4 kHz, No. of scans = 200, chemical shift standard TMS; for ^{27}Al, frequency = 78.17 MHz, pulse width = 0.7 μs, recycle time = 2 s,

spinning rate = 8 kHz, No. of scans = 400, chemical shift standard $Al(H_2O)_6^{3+}$.

2.4. EXAFS measurements and data reduction

The X-ray absorption measurements were performed at the Laboratoire pour l'Utilisation du Rayonnement Electromagnétique (Orsay, France) on the XAS2 beam line of the DCI storage ring operated at 1.85 GeV (320 mA). The X-rays were monochromatized in the Zn K region (9500–10 500 eV) by using a Si(311) two-crystal spectrometer. High order harmonics were rejected using a two-mirror device at 2 mrd incidence. Data were collected from Zn-exchanged zeolite and sodalite samples and from ZnO and $ZnAl_2O_4$ references in the transmission mode at low temperature (20 and 77 K). The incident and the transmitted intensities were measured with two ionization air-filled chambers. The thickness of the powders was adjusted in order to obtain a step-edge absorption $\Delta\mu \sim 1$.

The data were analyzed using the 'EXAFS pour le MAC' software [14]. The background absorptions above and below the Zn K-edge were subtracted by using polynomial functions. The oscillatory part of the EXAFS function $\chi(k)$ was determined as $\chi(k) = (\mu - \mu_0)/\mu_0$, where k is the photoelectron wave vector defined as $k = [2m(E - E_0)]^{1/2}/\hbar$. E is the photon energy and E_0 the threshold energy taken at the bottom of the edge, i.e. 9657 eV for all the samples. The EXAFS spectra were k^2-weighted and then Fourier-transformed over a k range of 2.5–12 $Å^{-1}$. The Fourier-filtered contributions of the first oxygen neighbor shells were simulated in single-scattering formalism using the phase shifts and backscattering amplitudes extracted from the analysis of a ZnO reference. For more distant shells, experimental and theoretical amplitude and phase shifts [15,16] were used in the calculations.

3. Results and discussion

3.1. XRD analysis

The XRD patterns of the as-synthesized and Zn-exchanged zeolites are shown in Fig. 2. The

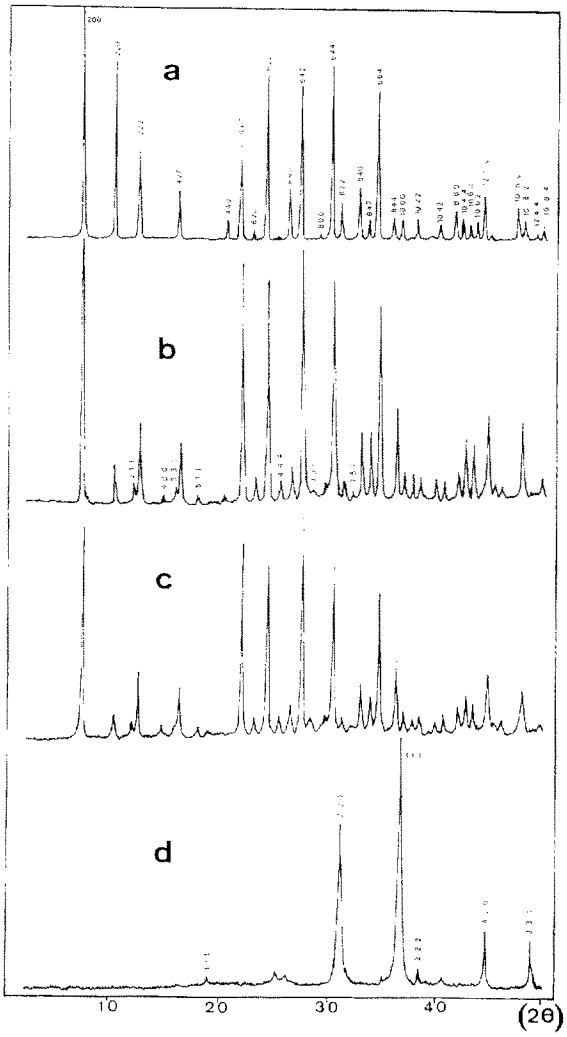

Fig. 2. XRD patterns of: (a) starting Na zeolite A; (b) Zn-exchanged zeolite A (AZEO80); (c) Zn-exchanged zeolite A calcined at 600 C (AZEO600); (d) $ZnAl_2O_4$ obtained from Zn-exchanged zeolite A heated at 850 C.

LTA-type zeolite crystallizes in the cubic symmetry ($a = 24.61$ Å) with the $Fm\bar{3}c$ space group [3]. The diffraction pattern of the Zn-exchanged AZEO80 sample [Fig. 2(b)] is similar to that of the starting LTA [Fig. 2(a)] with little change in the line intensities and slight shifts corresponding to a decrease in the a parameter down to 24.3 Å [8]. The additional reflections pointed out in Fig. 2(b) are indexable in the space group $Fm\bar{3}c$. They appear to be due to the replacement of sodium by zinc cations

[8]. The zeolite framework is not modified by the thermal treatment since the diffractogram of AZEO600 [Fig. 2(c)] is comparable to that of AZEO80. After calcination at 850 C [Fig. 2(d)], the reflections can be attributed to the $Fd3m$ space group. The XRD pattern corresponds to that of $ZnAl_2O_4$ ($a=8.086$ Å) [17].

The XRD patterns of the as-synthesized and Zn-exchanged sodalites are presented in Fig. 3. $Na_6Si_6Al_6O_{24}\cdot 8H_2O$ [Fig. 3(a)] crystallizes in the

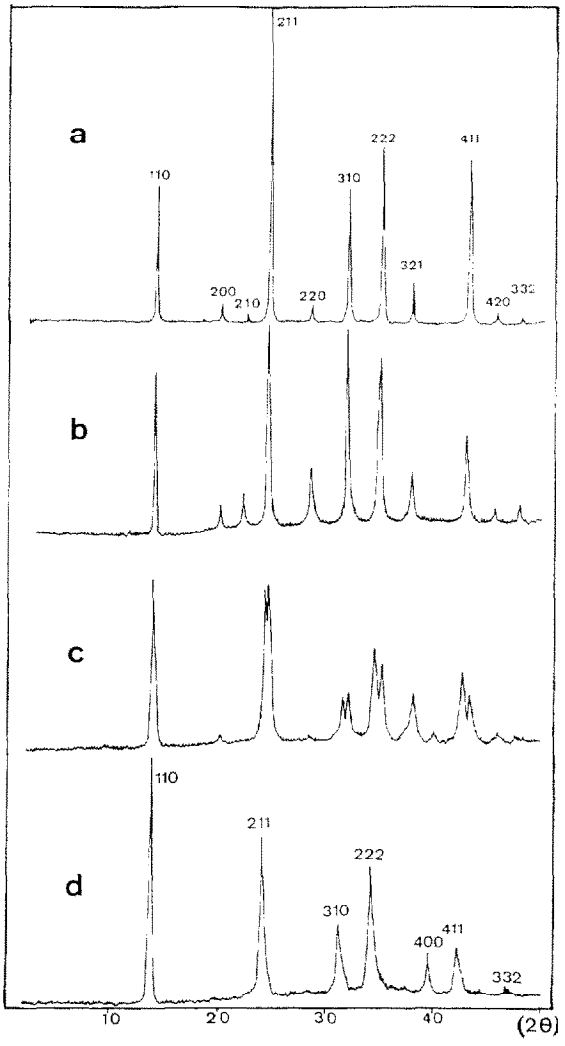

Fig. 3. XRD patterns of: (a) starting hydrosodalite; (b) partially Zn-exchanged sodalite (SOD80); (c) Zn-exchanged sodalite calcined at 400 C (SOD400); (d) Zn-exchanged sodalite calcined at 600 C (SOD600).

$P\bar{4}3n$ space group with $a=8.85$ Å [18]. SOD80 [Fig. 3(b)] presents a similar XRD pattern with a small shift of the lines corresponding to a slightly increased parameter $a=8.97$ Å. After calcination, the lines of SOD400 are broadened and split [Fig. 3(c)]. In SOD600 [Fig. 3(d)], the (200), (210), (220), and (321) lines disappear whereas the (400) line appears. The intensities of some lines are modified. The a parameter increases to the value $a=9.09$ Å. It may be assumed that SOD400 is not a pure phase, because the change on calcination of SOD80 was not complete, in contrast to sample SOD600, for which the transformation may be considered to be complete.

3.2. Solid-state NMR spectroscopy

^{29}Si MAS NMR provides information on the modifications of the zeolite framework [19]. There is no marked difference between the ^{29}Si solid-state MAS NMR spectra of LTA Na before [Fig. 4(a)] and after Zn-exchange [AZEO80, Fig. 4(b)] and thermal treatment [AZEO600, Fig. 4(c)]. The chemical shift is -89.2 ppm in each case and the linewidth increases from 1.6 ppm to 2.2 and 2.7 ppm for AZEO80 and AZEO600, respectively. Therefore, the zeolite framework is only slightly affected by Zn-exchange and thermal treatments. The ^{29}Si solid-state MAS NMR spectrum of the starting sodalite [Fig. 4(d)] shows a large peak centered at -85.2 ppm. In the case of sodalites, it is known that the resonance frequency is related to the $Si(OAl)_4$ tetrahedron and linearly dependent on the lattice parameter and may vary from -77 ppm to -91 ppm [20]. The measured chemical shift is in fair agreement with the expected chemical shift for a lattice parameter of 8.85 Å, according to ref. [20]. The partial exchange of Na^+ by Zn^{2+} ions results in a splitting of the peak [Fig. 4(c)]: the geometry of a part of the $Si(OAl)_4$ tetrahedra is modified by the treatment. After calcination [SOD600, Fig. 4(f)], a broad peak is observed.

The ^{27}Al MAS NMR spectra of the starting Na-A [Fig. 5(a)], AZEO80 [Fig. 5(b)] and AZEO600 [Fig. 5(c)] are quite different. Only a narrow peak at 57.4 ppm, which is attributed to

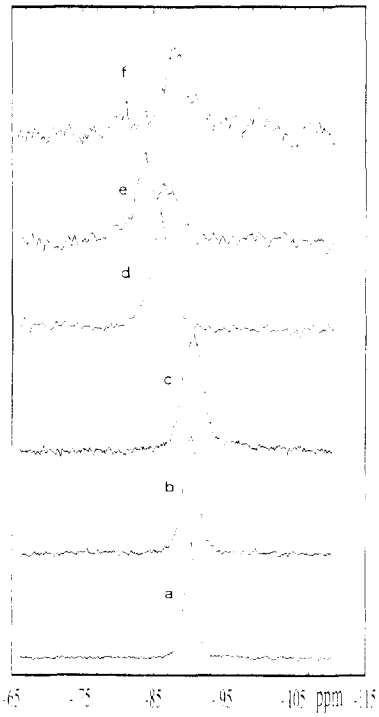

Fig. 4. ^{29}Si MAS NMR spectra of (a) starting Na zeolite A; (b) Zn-exchanged zeolite A (AZEO80); (c) Zn-exchanged zeolite A calcined at 600 C (AZEO600); (d) starting hydrosodalite; (e) partially Zn-exchanged sodalite (SOD80); (f) Zn-exchanged sodalite calcined at 600 C (SOD600).

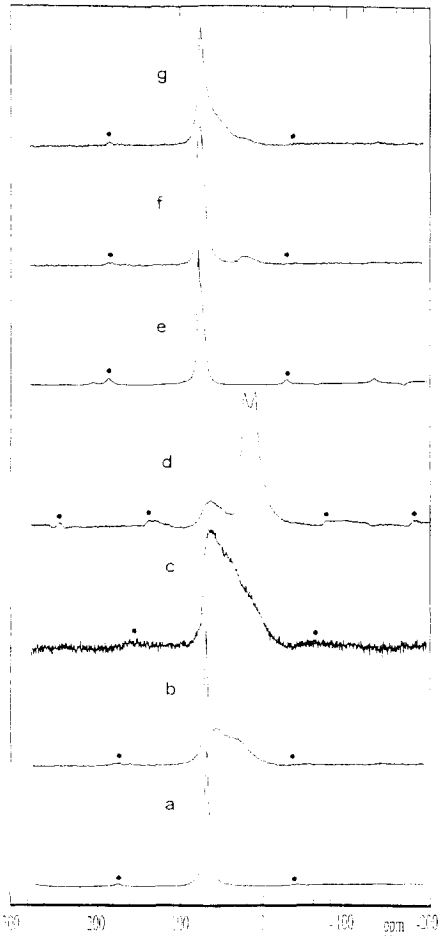

Fig. 5. ^{27}Al MAS NMR spectra of (a) starting Na zeolite A; (b) Zn-exchanged zeolite A (AZEO80); (c) Zn-exchanged zeolite A calcined at 600 C (AZEO600); (d) $ZnAl_2O_4$ obtained from Zn-exchanged zeolite A heated at 850 C; (e) starting hydrosodalite; (f) partially Zn-exchanged sodalite (SOD80); (g) Zn-exchanged sodalite calcined at 600 C (SOD600).

aluminum belonging to the zeolite framework, is observed for the starting material, in agreement with previous results [19]. After Zn-exchange [AZEO80, Fig. 5(b)], a broad shoulder is observed on the low chemical shift side of the main peak, with a maximum at about 30 ppm. This indicates that for most of the aluminum atoms present in the framework, the surrounding is greatly modified by Zn-exchange. After calcination, the whole spectrum is broadened [Fig. 5(c)], but the fingerprint of $ZnAl_2O_4$ does not appear. The spectrum of the last compound [Fig. 5(d)] is characterized by a doublet signal at about 10 ppm, which is a typical quadrupolar pattern representing a single octahedral aluminum site [19]. The high-field shoulder of the spectrum in Fig. 5(c) may arise partly from less well crystallized $ZnAl_2O_4$ and partly from distorted framework aluminum. The spectrum of the starting sodalite [Fig. 5(e)] presents a single peak at 60 ppm in agreement with previous work [19,21]. After Zn-exchange [SOD80, Fig. 5(f)], the peak is broadened. The presence of an additional weak peak around 10 ppm can be assigned to a small amount of extra-framework aluminum in octahedral coordination [19]. After heating [SOD600, Fig. 5(g)], a broad shoulder appears on the low chemical shifts side of the main peak, showing again that some distortions occur in the tetrahedral Al environment.

3.3. EXAFS results and discussion

The results of the simulations are summarized in Table 1. For the zeolite sample the Debye–Waller σ values reported in Table 1 are relative to ZnO for the Zn–O and Zn–Zn pairs, and absolute for the Zn–Al one. The maximum number of fitting parameters is limited by the number of independent data points. $N_{ind} = 2\Delta k \Delta R/\pi$, where Δk and ΔR are respectively the widths in k and R space used in the fit. The uncertainty reported in Table 1 was obtained from the variation of the parameter that gives twice the maximum residue.

The $k\chi(k)$ data recorded from Zn-exchanged zeolite and sodalite samples are shown in Fig. 6 along with the spectra of $ZnAl_2O_4$ and ZnO. The main oscillation is due to oxygen first neighbors of Zn and has the same wavenumber in all the samples. The Fourier transforms of the $k^2\chi(k)$ shown in Fig. 7 confirm that the first neighbors' peak has approximately the same position in the zeolite A and sodalite samples as in the references. In ZnO [22], Zn is at the center of a slightly distorted tetrahedron with three Zn–O distances of 1.97 Å and one of 1.99 Å. The average of the four Zn–O distances in $ZnAl_2O_4$ is 1.95 Å. The EXAFS study of the references is described in detail in ref. [23].

Table 1
Structural parameters deduced from the analysis of the first, second and third neighbor shells of zinc in reference samples and Zn-exchanged zeolite A and sodalite submitted to thermal treatments. Debye–Waller σ parameters are related to ZnO

Compound	Pair	R (Å)	N	σ (Å)
ZnO	Zn–O	1.97±0.01	4.1±0.3	0.00
	Zn–Zn	3.24±0.01	12±1	0.00
ZnAl2O4	Zn–O	1.95±0.02	4.0±0.4	0.00
	Zn–Al	3.36±0.02	12±3	0.00
	Zn–Zn	3.52±0.02	4±1	0.00
AZEO80	Zn–O	1.97±0.01	4.1±0.3	0.06±0.02
	Zn–Zn	3.31±0.02	2.0±0.3	0.05±0.02
AZEO540	Zn–O	1.97±0.01	4.0±0.2	0.05±0.01
	Zn–Zn	3.31±0.02	2.1±0.3	0.07±0.02
AZEO600	Zn–O	1.98±0.01	4.0±0.3	0.06±0.02
	Zn–Zn	3.30±0.02	2.0±0.3	0.07±0.02
SOD80	Zn–O	2.07±0.01	4.0±0.3	0.08±0.02
	Zn–Zn	3.09±0.02	1.4±0.3	0.02±0.02
SOD400	Zn–O	1.95±0.01	4.1±0.2	0.05±0.02
	Zn–Zn	3.30±0.02	1.3±0.3	0.06±0.02
SOD600	Zn–O	1.95±0.01	4.0±0.3	0.02±0.01
	Zn–Al	2.86±0.02	2.0±0.4	0.10±0.02
	Zn–Zn	3.39±0.02	1.3±0.3	0.05±0.02

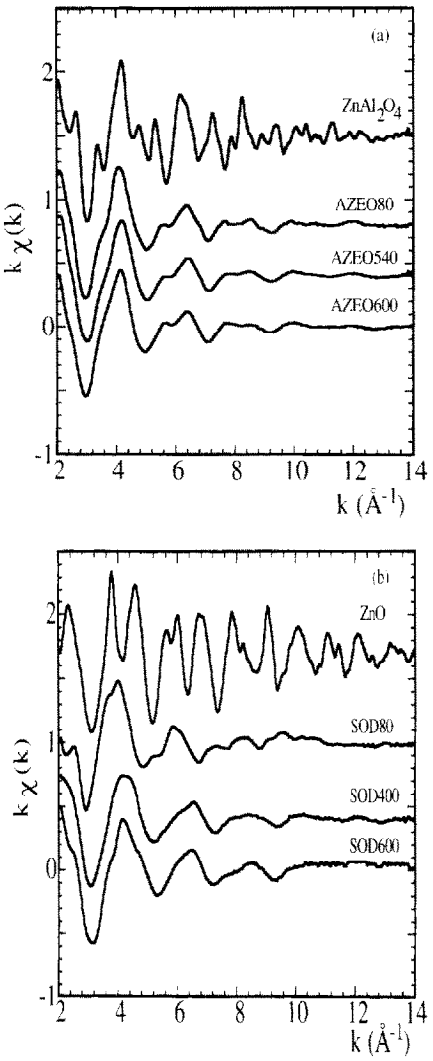

Fig. 6. $k\chi(k)$ EXAFS spectra at the Zn K-edge recorded from: (a) Zn-exchanged LTA zeolites and $ZnAl_2O_4$; (b) partially Zn-exchanged sodalite and ZnO.

The results of the simulations (Table 1 and Fig. 8) confirm that there is no marked difference between the first oxygen neighbor environment in the various samples. In exchanged A-zeolites and sodalites, whatever the treatment, the Zn cations

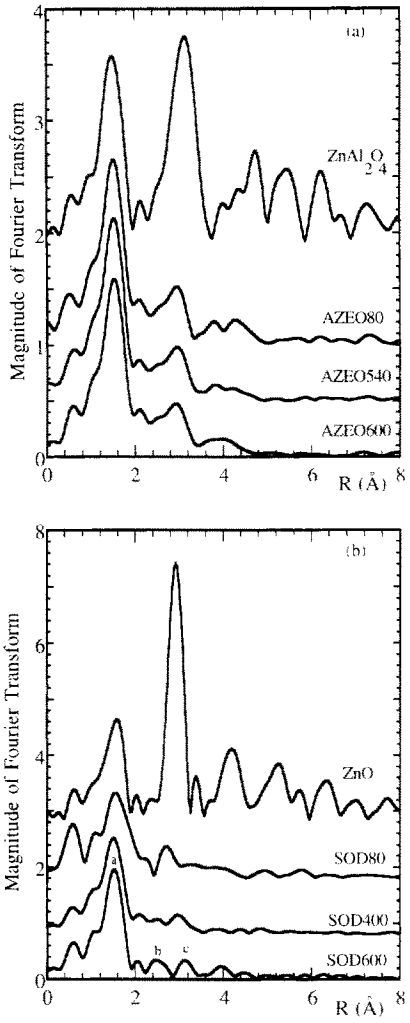

Fig. 7. Fourier transforms of $k^2\chi(k)$ data recorded from: (a) Zn-exchanged LTA zeolites and $ZnAl_2O_4$; (b) partially Zn-exchanged sodalite and ZnO. The curves are presented without phase shifts corrections.

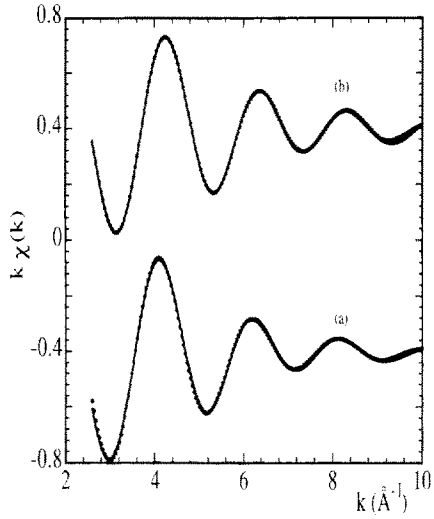

Fig. 8. Best fits of the Fourier filtered contribution of the first neighbors with the parameters shown in Table 1 for (a) Zn-exchanged zeolite A calcined at 600 C (AZEO600); (b) partially Zn-exchanged sodalite calcined at 600 C (SOD600): experiment (dots), calculation (full line).

are four-fold coordinated with oxygen with a mean Zn–O distance of 1.97 Å (excepted in the SOD80 sample), a value close to that found in the ZnO and $ZnAl_2O_4$ references. The four Zn–O distances are essentially the same, though the distortion of the first coordination shell is more marked than in the reference samples, as shown by the high σ values (Table 1). The strongest distortion is observed for the SOD80 sample. However, the high values of the σ parameter with respect to the crystalline references show that the ZnO_4 tetrahedra are located in several sites more or less distorted. The calcination improves the regularity of the tetrahedra, especially for sodalites where σ decreases on increasing the calcination temperature (Table 1).

Above 2 Å (Fig. 7), the FTs of the various samples show a smaller amplitude compared with the reference samples, which confirms the loss of local order observed in the first coordination shell of Zn. This observation is consistent with XRD that shows the absence of crystalline ZnO (or $ZnAl_2O_4$) in the samples. Moreover, inspection of the FTs for the zeolite and sodalite samples between 2 and 4 Å reveals some differences between them, which indicate a change in the structure of the zinc oxide particles.

In order to derive structural information from the second and third coordination shells in Zn-exchanged zeolite and sodalite samples, the reference samples were carefully investigated [23]. In hexagonal ZnO, Zn^{2+} ions have six Zn neighbors at 3.21 Å and six others at 3.25 Å, which gives 12 Zn neighbors at a mean distance of 3.23 Å. In addition, Zn atoms have one oxygen neighbor located at 3.215 Å. These atoms can be involved

in multiple scattering (MS) paths of the photoelectron, which contribute to the EXAFS signal. In order to check the validity of the single-scattering formalism for the treatment of the zeolite A and sodalite data, the ab initio multiple scattering X-ray absorption code FEFF [16] was used to perform XAFS calculations including SS and MS paths above 5 Å. The MS approach will be discussed in detail in ref. [24]. The results show that above 5 $Å^{-1}$, the contribution of MS to EXAFS is negligible [24]. Therefore, simulations were performed in single-scattering formalism on the Fourier-filtered contributions of the peaks located between 2.2 and 3.5 Å in the FT. The results of the simulations of the Fourier-filtered contribution above 5 $Å^{-1}$ of the ZnO second neighbor peak (Table 1) are in agreement with the values derived from crystallography. On the other hand, in $ZnAl_2O_4$, Zn^{2+} has 12 Al neighbors at 3.35 Å and four Zn neighbors at 3.50 Å [17]. Both contribute to the large peak located between 2.4 and 3.7 Å in the FT [Fig. 7(a)] and are well resolved in a two-shells fit (Table 1 and ref. [23]).

Let us consider the FT of the Zn-exchanged A-zeolite samples [Fig. 7(a)]. The shape of the FT of EXAFS data recorded from all of them exhibit a double-peaked structure between 2.3 and 3.7 Å similar to that of $ZnAl_2O_4$, though its amplitude is lower. However, the maximum of the peak at 3.1 Å corresponding to the third Zn neighbor in $ZnAl_2O_4$ is shifted to lower R values. This observation reveals a mixing of several Zn environments and is consistent with the results of other characterizations. The peak is well accounted for by Zn neighbors at 3.31 Å, which is intermediate between the Zn–Zn distances in ZnO and $ZnAl_2O_4$. Attempts to include Al neighbors in the fits failed. The EXAFS spectra result from the contribution of inequivalent Zn^{2+} cations belonging to either clusters of different size located in the sodalite cages and α-cages [6].

The FTs of $k\chi(k)$ data recorded from sodalite samples look quite different above 2.2 Å [Fig. 7(b)]. It is noteworthy that two well separated peaks, labelled b and c in Fig. 7(b), appear at 2.5 and 3.1 Å in the FT of SOD600. While the amplitude of the Fourier-filtered envelope of the former (b) is consistent with Al or Si surrounding, the latter is assigned to Zn neighbors. Ranges and details of the Fourier-filtered calculation are given in ref. [24]. The mean Zn–Al(Si) and Zn–Zn distances are 2.86 Å and 3.39 Å, respectively, whereas the number of Zn backscatterers is about two (Table 1). The best fits of the second (Al,Si) and third (Zn) neighbors contribution in the k-space are shown in Fig. 9(a) for (Al,Si), for Zn in Fig. 9(b) and in Fig. 9(c) for the peaks together. The short distance between Zn^{2+} ions belonging to the clusters and Al belonging to the sodalite framework (with respect to the Zn–Al distance in $ZnAl_2O_4$) can be attributed to the attraction of the negative charge of the cage. The short distance between Zn^{2+} and framework Al^{3+} is not surprising, since the ^{29}Si and ^{27}Al NMR spectra reveal strong modifications in the aluminum environment (see above). EXAFS cannot distinguish between Al or Si backscatterers, but NMR spectra as well as considerations on the charge effects in the framework allow us to assign Al^{3+} ions as second neighbors of Zn^{2+}. Moreover, the mean Zn–Zn distance in SOD600 is longer than in bulk ZnO and Zn-exchanged zeolite A. This result shows again that Zn^{2+} cations are located as close as possible to the wall of the cages. The same conclusions can be inferred from the data recorded on sodalite dried at 400°C. However, in SOD400, XRD revealed the mixture of two phases (see above) and, accordingly, several Zn environments, especially if lower calcination temperatures were used.

Therefore, the strong interaction between Zn^{2+} cations located in the cages of the Zn-exchanged sodalite is indicated by EXAFS since short Zn–Al distances are clearly established after calcination. This result is in agreement with previous single-crystal XRD study of Zn-exchanged zeolite A which revealed that the first neighbor environment of a part of Zn^{2+} located in the sodalite cages is formed by three bonds with oxygen atoms of the framework and one bond with a non-framework oxygen [6].

It was demonstrated that M_4X tetrahedra like $(Zn_4Se)^{6+}$ tetrahedra can be stabilized in the cages of borate sodalite with a central anion X surrounded by four M cations in a tetrahedral arrangement [4]. In the present case, the M_4X

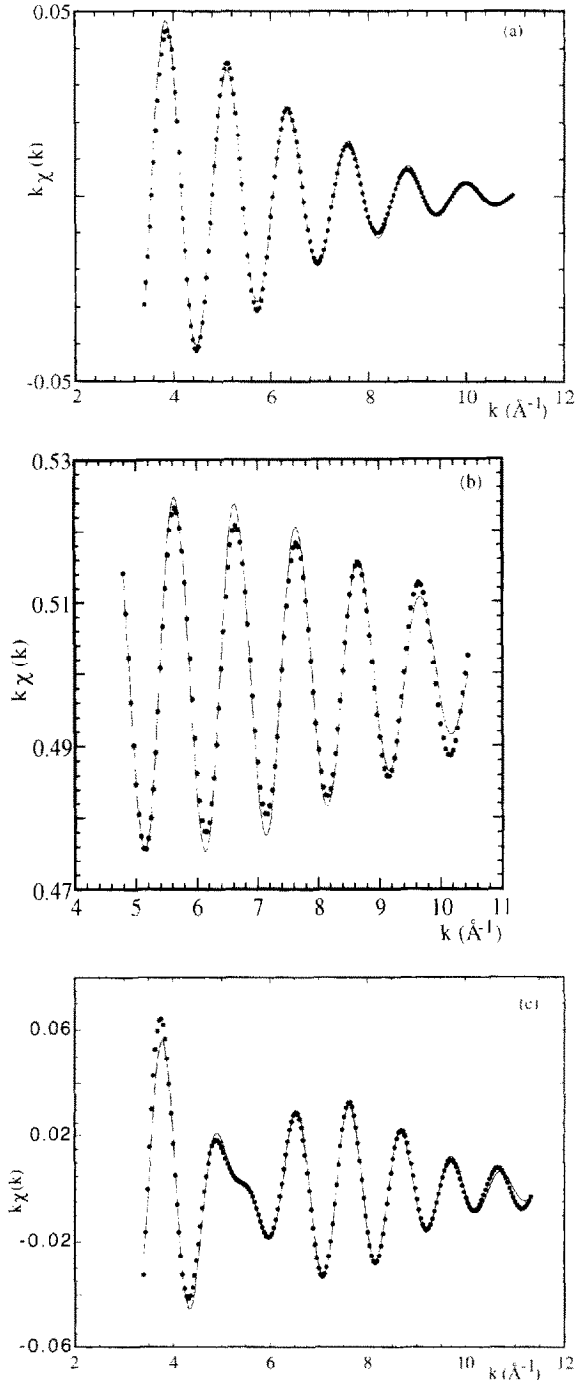

Fig. 9. Best fits of the Fourier filtered contribution of the (a) second (Al), (b) third (Zn) neighbors contribution and (c) both contributions of Al and Zn with the parameters shown in Table 1 for partially Zn-exchanged sodalite calcined at 600 C (SOD600): experiments (dots), calculations (full line).

tetrahedra should be formed by $(Zn_4O)^{6+}$ cations [8], keeping in mind that the ionic radius is 1.40 Å for oxygen instead of 1.98 Å for selenium. The short distance deduced from EXAFS between Zn^{2+} ions and Al^{3+} belonging to the framework allows us to rule out the formation of such polycations in sodalite cages. On the other hand, if clusters of the $(Zn_4O)^{6+}$ type were located at the center of the cage (about 6 Å in diameter), the three Zn–O bonds with oxygen of the framework should be longer (about 2.5 Å) [25]. The occurrence of such clusters in the cages can be considered if the radii of the inserted atoms are big enough to fill the sodalite cage, as observed for ZnSe particles in borate sodalites [4]. Moreover, the charge of the aluminosilicate framework is -3 per cage instead of -6 for the borate cage, and the charge compensation would not be achieved.

The number of Zn neighbors of Zn is less than two (Table 1). This may correspond either to three zinc cations present in part of the sodalite cages, the other cages containing essentially Na^+ cations, or to three zinc cations located in three adjacent cages, each of them being close to a common six-membered ring. The hydrolysis of Zn^{2+} during and after the exchange reaction [8,13] would reduce the positive charge of the clusters and explain the charge compensation by zinc cations instead of sodium cations. The second model is also consistent with the Zn–Zn distances and coordination numbers determined by EXAFS.

4. Conclusion

The study of the atomic structure of zinc oxide particles in Zn-exchanged sodalite and zeolite A shows that zinc ions are tetracoordinated to oxygen. It is not possible to draw an inference from this study on the structure of the particles inserted in the sodalite cages of Zn-exchanged zeolite A, since the EXAFS spectra result in the present case from the contribution of inequivalent Zn cations belonging to clusters of different size located either in the sodalite cages or the α-cages. In Zn-exchanged sodalites, after calcination at 600 C, the second shell of neighbors around Zn consists of Al^{3+} cations belonging to the frame-

work. The zinc cations are located very close to the wall of the sodalite cage, i.e. chemisorbed on the framework since they engage short bonds with oxygen and aluminum of the framework and longer ones with zinc. The third neighbors of Zn consist of at most two zinc cations at 3.39 Å. The results are consistent with the adsorption on the sodalite framework of clusters involving three Zn cations probably hydrolyzed and belonging either to the same cage or to three adjacent cages.

Acknowledgement

The authors thank the staff of the Laboratoire pour l'Utilisation du Rayonnement Electromagnétique for their assistance during the X-ray absorption experiments. L. Khouchaf would like to thank the Ecole Supérieure des Techniques Industrielles et des Mines de Douai for financial support. M. Wark is grateful for a postdoctoral fellowship by the French Ministère des Affaires Etrangères. Dr. J.L. Paillaud is greatly acknowledged for computer modeling.

References

[1] J.A. Rabo, in: J.A. Rabo (Ed.), Zeolite Chemistry and Catalysis, ACS Monograph 171, American Chemical Society, Washington, DC, 1976.
[2] D.W. Breck, Zeolite Molecular Sieves, Wiley, New York, 1974.
[3] W.M. Meier, D.H. Olson, Atlas of Zeolite Structure Types, Butterworth-Heinemann, Stoneham, USA, 1992.
[4] K.L. Moran, T.E. Gier, W.T.A. Harrison, G.D. Stucky, H. Eckert, K. Eichele, R.E. Wasylishen, J. Am. Chem. Soc. 115 (1993) 10553.
[5] Y. Kim, K. Seff, J. Phys. Chem. 84 (1980) 2823.
[6] L.B. McCusker, K. Seff, J. Phys. Chem. 85 (1981) 405.
[7] T. Türk, F. Sabin, A. Vogler, Mater. Res. Bull. 27 (1992) 1003.
[8] M. Wark, W. Lutz, E. Löffler, H. Kessler, G. Schulz-Ekloff, in: J. Weitkamp, H.G. Karge, H. Pfeifer, W. Hölderich (Eds.), Zeolites and Related Microporous Materials: State of the Art 1994, Studies in Surface Science and Catalysis, Vol. 84, 1994, p. 1043.
[9] M. Wark, G. Schulz-Ekloff, N.I. Jaeger, Catal. Today 8 (1991) 467.
[10] G.A. Ozin, Adv. Mater. 4 (1992) 612.
[11] K. Moller, M.M. Eddy, G.D. Stucky, N. Herron, T. Bein, J. Am. Chem. Soc. 111 (1989) 2564.
[12] L. Khouchaf, M.-H. Tuilier, J.-L. Guth, B. Elouadi, J. Phys. Chem. Solids 57 (1996) 251.
[13] M. Wark, W. Lutz, G. Schulz-Ekloff, A. Dyer, Zeolites 13 (1993) 658.
[14] A. Michalovicz, Logiciels pour la Chimie, Société Française de Chimie, Paris, 1991, p. 102.
[15] A.G. McKale, B.W. Veal, A.P. Paulikas, S.K. Chan, G.S. Knapp, J. Am. Chem. Soc. 110 (1988) 3763.
[16] J. Mustre de Leon, J.J. Rehr, S.I. Zabrinsky, R.C. Albers, Phys. Rev. B 44 (1991) 4146.
[17] P. Fischer, Z. Kristallogr. 124 (1967) 275.
[18] G. Engelhardt, J. Felsche, P. Sieger, J. Am. Chem. Soc. 114 (1992) 1173.
[19] G. Engelhardt, D. Michel, High Resolution Solid-state NMR of Silicates and Zeolites, Wiley, Chichester, 1987.
[20] M.T Weller, G. Wong, J. Chem. Soc., Chem. Commun. (1988) 1103.
[21] H.S. Jacobsen, P. Norby, H. Bildsoe, H.J. Jakobsen, Zeolites 9 (1989) 491.
[22] S.C. Abraham, J.L. Bernstein, Acta Crystallogr. B25 (1969) 1233.
[23] L. Khouchaf, M.-H. Tuilier, J. Dürr, M. Wark, H. Kessler, J. Phys. IV 6 (1996) C4–939.
[24] L. Khouchaf, M.-H. Tuilier, M. Wark, J. L. Paillaud, M. Soulard, J. Phys., in press.
[25] J.L. Paillaud, Personal communication.